

# Virtual Transmission Solution Based on Battery Energy Storage Systems to Boost Transmission Capacity

Matías Agüero, *Student Member, IEEE*, Jaime Peralta, *Member, IEEE*, Eugenio Quintana, Victor Velar, *Member, IEEE*, Anton Stepanov, *Member, IEEE*, Hossein Ashourian, *Member, IEEE*, Jean Mahseredjian, *Fellow, IEEE*, and Roberto Cárdenas, *Senior Member, IEEE*

**Abstract**—The increasing penetration of variable renewable energy (VRE) generation along with the decommissioning of conventional power plants in Chile, has raised several operational challenges in the Chilean National Power Grid (NPG), including transmission congestion and VRE curtailment. To mitigate these limitations, an innovative virtual transmission solution based on battery energy storage systems (BESSs), known as grid booster (GB), has been proposed to increase the capacity of the main 500 kV corridor of the NPG. This paper analyzes the dynamic performance of the GB using a wide-area electromagnetic transient (EMT) model of the NPG. The GB project, composed of two 500 MVA BESS units at each extreme of the 500 kV corridor, allows increasing the transmission capacity for 15 min during  $N-1$  contingencies, overcoming transmission limitations under normal operation conditions while maintaining system stability during faults. The dynamic behavior of the GB is also analyzed to control power flow as well as voltage stability. The results show that the GB is an effective solution to allow greater penetration of VRE generation while maintaining system stability in the NPG.

**Index Terms**—Battery energy storage system (BESS), grid booster, transient stability, voltage stability, electromagnetic transient (EMT).

## I. INTRODUCTION

THE development and operation of the Chilean National Power Grid (NPG) are undergoing significant changes due to the increasing penetration of variable renewable energy (VRE) generation, creating numerous challenges for Coordinador Eléctrico Nacional (CEN), the Chilean electric sys-

tem operator [1]. The installed VRE generation capacity in Chile was 11936 MW in 2022, very similar to the peak demand (11906 MW) observed in the same year, and the VRE generation share was 28%. This trend is expected to continue and deepen in future, with energy levels of VRE reaching up to 85% by the end of the decade. The challenges of the energy transition are magnified by the radial topology and extended nature of the NPG, spanning over 3000 km, with VRE resources at remote locations, far from the main load centers [2].

CEN is committed to facilitating the energy transition and the goal of reaching carbon neutrality by 2050, contributing to the development of a sustainable power grid in Chile. As part of this vision, a roadmap has been developed to phase out all coal-based power plants and achieve a 100% share of renewable generation by 2030 [3]. The grid of the future shall safely and reliably accommodate the integration of new emerging technologies such as the grid booster (GB) project [4] into the NPG. To achieve this goal, it is crucial to conduct in-depth analysis and to review the technical requirements for inverter-based resources (IBRs) specified in the Chilean grid code [5].

The GB, also referred to as virtual transmission solution based on battery energy storage systems (BESSs), has the potential to increase power export capability without necessitating the construction of new transmission lines [6], [7]. The GB project proposed by the regulator in Chile [8] is comprised of two 500 MVA, 125 MWh BESS units: one is located in the northern part of the Chilean NPG at Parinas substation, near a solar generation cluster, and the other is located in the central part of the Chilean NPG at Lo Aguirre substation, near Santiago, as shown in Fig. 1. The two BESS units operate in a coordinated manner injecting and absorbing energy during contingencies along the Parinas–Lo Aguirre 500 kV corridor.

Historically, root mean square (RMS) or phasor domain transient (PDT) simulations have been the standard methods to study the dynamic behavior of power systems composed primarily of synchronous generators (SGs) [9]. However, with the increased presence of IBRs, the need to account for new dynamics associated with controllers and power electronic components has become evident [10]–[12], raising the

Manuscript received: September 30, 2023; revised: January 27, 2024; accepted: February 20, 2024. Date of CrossCheck: February 20, 2024. Date of online publication: March 30, 2024.

This article is distributed under the terms of the Creative Commons Attribution 4.0 International License (<http://creativecommons.org/licenses/by/4.0/>).

M. Agüero (corresponding author), J. Peralta, E. Quintana, and V. Velar are with Coordinador Eléctrico Nacional, Santiago, Chile (e-mail: matias.aguero@coordinador.cl; jaime.peralta@coordinador.cl; eugenio.quintana@coordinador.cl; victor.velar@coordinador.cl).

A. Stepanov and H. Ashourian are with PGSTech, Montreal, Canada (e-mail: anton.stepanov@emtp.com; hossein.ashourian@emtp.com).

J. Mahseredjian is with École Polytechnique de Montréal, Montréal, Canada (e-mail: jean.mahseredjian@polymtl.ca).

R. Cardenas is with University of Chile, Santiago, Chile (e-mail: rcardenas@ing.uchile.cl).

DOI: 10.35833/MPCE.2023.000729



need to incorporate more advanced time domain or electro-magnetic transient (EMT) simulation tools. For this reason, CEN has undertaken an effort to build an EMT model of the Chilean NPG (EMT-NPG) to simulate the transient and dynamic behavior of the system under very high penetration levels of VRE generation [13]. A comprehensive wide-area EMT database was constructed for the NPG in EMTP<sup>®</sup> software [14].

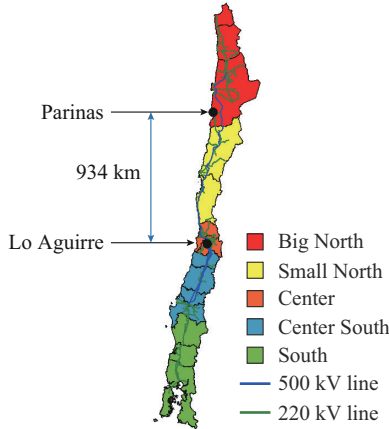


Fig. 1. Chilean NPG segmented by voltage control areas (VCAs).

The EMT-NPG database encompassed the modeling of all transmission lines in the bulk grid (220 kV and 500 kV), generation plants above 20 MW, and relevant dynamic voltage control devices. Furthermore, given their significance in voltage stability, the metal oxide varistor (MOV) systems associated with the series capacitors along the primary 500 kV corridors were also incorporated into the model.

The main contribution of this paper is the detailed modeling and validation of the design and dynamic performance of GB project in a large-scale EMT-NPG. This project is the first real-world application of this type and scale. In addition, the full GB model, including BESS and control schemes, was developed and integrated into a wide-area EMT database for accurate and detailed stability analysis.

The rest of this paper is organized as follows. Section II describes the main characteristics of the Chilean NPG and its EMT representation. Section III presents the GB project configuration, main parameters, and EMT model. Section IV presents the simulation results. Finally, the conclusions are presented in Section V.

## II. MAIN CHARACTERISTICS OF CHILEAN NPG AND ITS EMT REPRESENTATION

The Chilean NPG is characterized by its extended and islanded topology representing a complex operational configuration as we transition to a 100% renewable scenario, mostly dominated by IBRs. The peak demand in 2022 reached 11.9 GW, which was supplied by an installed capacity of 33 GW, encompassing a diverse mix of thermal (41%) and renewable energy (59%) generation sources. The Chilean NPG is characterized by five VCAs, corresponding to distinct geographical regions: Big North, Small North, Center, Center South, and South, as shown in Fig. 1. The installed capacity

and demand in each VCA are detailed in Table I.

TABLE I  
INSTALLED CAPACITY AND DEMAND IN EACH VCA

VCA	Demand (GW)	Installed capacity (GW)			
		Solar	Wind	Hydro	Thermal
Big North	2.7	3.3	0.9	<0.1	4.7
Small North	1.1	2.5	1.6	<0.1	0.8
Center	3.5	0.8		1.0	3.0
Center South	2.5	0.9	0.9	5.6	1.0
South	0.7		1.2	0.6	
Total	10.5	7.5	4.6	7.3	9.5

In recent years, the Chilean NPG has significantly evolved, facing multiple changes including:

- 1) Closure of thermal generators: closure of several thermal generators throughout the system.
- 2) Construction of VRE: construction of large-scale solar and wind power plants in the northern region.
- 3) Congestion in transmission corridors: congestion of the main transmission lines connecting the North (Big North and Small North) area, where solar and wind generation systems are concentrated, and the Center area, where a significant portion of demand is located. This issue has resulted in curtailment of VRE generation in both the Big North and Small North areas.

All these changes in the Chilean NPG have raised a need for innovative solutions to increase transmission capacity in a cost-efficient manner while maintaining grid stability. Despite the long-term strategies being considered, urgent short-term measures are required to address immediate challenges and constraints in the grid. The capacity of the Parinas–Lo Aguirre 500 kV corridor, a 1100 km heavily compensated transmission system, is 1700 MVA, which is primarily driven by voltage stability constraints. Thus, the need to increase power flow transfers in this corridor has become critical to reduce VRE curtailments. Innovative solutions such as the GB project aim at alleviating this constraint by temporarily increasing the transmission capacity during faults while maintaining system stability.

The complexities of Chilean NPG, combined with the country's ambitious goal for VRE integration, demand a holistic and forward-thinking approach to grid development and management of operations. The intricate interactions between VRE, conventional generation technologies, and transmission infrastructure necessitate advanced simulation tools and novel solutions like the GB project.

This study considers two daytime-peak operation scenarios projected for the year 2025, under conditions of the maximum instantaneous VRE penetration, covering a capacity of 400 MW or 500 MW for the BESS units due to the requirements of the project. Table II shows the main parameters of the two scenarios represented in the EMT-NPG, where NPA denotes for Nueva Pan de Azucar.

The EMT-NPG used in this paper corresponds to the first version of an EMT representation of the Chilean NPG developed in EMTP<sup>®</sup> [14]. The modeling characteristics of the main components in the EMT-NPG are described as follows.

TABLE II  
MAIN PARAMETERS OF TWO SCENARIOS

Parameter	Scenario 1	Scenario 2
Total generation	10437.0 MW	10522.4 MW
VRE generation	6787.2 MW	6962.6 MW
Total load	9991.9 MW	10136.9 MW
Loss	445.51 MW	385.4 MW
The maximum power transfer (NPA–Polpaico)	2444.2 MW	2377.2 MW
BESS/VRE ratio	7.37%	7.18%

### A. SGs

The EMT-NPG is composed of 62 SGs, which are modeled considering salient-pole single-mass for the thermal units, and round rotors for the hydro units. All machines are modeled with their excitation, power stabilizers, and governor's systems [15].

### B. Wind Parks and Solar Plants

The model is composed of 32 wind parks and 59 solar plants. VRE generators have been reproduced from the models available in the phasor-domain tool used by CEN, and Generic Western Electricity Coordinating Council (WECC) models [16], available in the EMT<sup>®</sup> Renewables library, have been used for future VRE plants. In the case of wind parks, both full converter and doubly-fed induction generator (DFIG) models were used [17], [18].

### C. Transmission Lines

The model includes 678 transmission lines consisting of 500 kV, 220 kV, and 110 kV lines. Lower voltage levels are represented by aggregated equivalent loads. Lines longer than 10 km are represented by distributed parameter models with constant parameters [19]. Short lines are represented by concentrated  $\pi$  sections due to the time-step restrictions. All series capacitors in the 500 kV corridor are modeled with their corresponding MOV arresters with nonlinear  $V$ - $I$  characteristics.

## III. GB PROJECT CONFIGURATION, PARAMETERS, AND EMT MODEL

The GB project is located between the Parinas and Lo Aguirre 500 kV substations. Its primary aim is to increase the power transfers along the 500 kV corridor between the Parinas and Lo Aguirre substations, to allow exceeding the normal  $N-1$  capacity in this corridor by 400-500 MW. This is achieved through dynamic active power compensation, delivered by two 500 MVA BESS units installed at each substation. Thus, in case of losing one line circuit, the BESS units will simultaneously absorb (and inject) energy at the two extremes of the corridor to compensate for the excess of power transfer to avoid exceeding the limit of the healthy circuit. The general specifications of the GB project (size and duration) analyzed in this paper, are defined based on the current level of VRE curtailments due to transmission constraints in the 500 kV corridor of the NPG.

### A. GB Control System

The BESS units shall be coordinated utilizing a redundant high-speed communication and control system, which incorporates a central control system (CCS) and a power plan controller (PCC) at each BESS site [20]. The CCS is critical for achieving the necessary speed and precision for a safe, reliable, and coordinated operation. The GB will have two main operation modes as follows.

1) Normal operation mode: during normal operation mode, considering the power transfers from the North to the South, the systems maintain an operational setting of the minimum state of charge (SoC) for the BESS unit at Parinas substation (BESS 1) and the maximum SoC for the BESS unit at Lo Aguirre substation (BESS 2), as shown in Fig. 2.

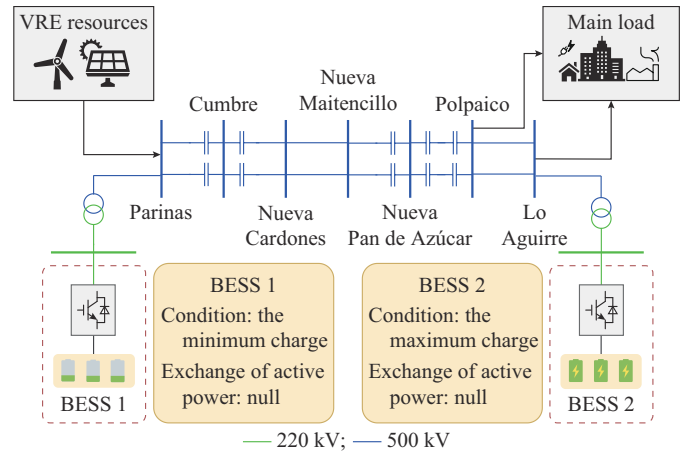


Fig. 2. Schematic diagram of normal operation mode.

2) Contingency operation mode: if a fault occurs at one of the circuit sections along the 500 kV corridor, causing the loss of the faulted line, both BESS units shall operate in a coordinated manner to maintain the pre-fault power flow balance without overloading the parallel healthy line. This is achieved by simultaneously charging (absorbing energy) BESS 1 and discharging (injecting energy) BESS 2, minimizing the impact on the grid without violating grid code requirements. This operation mode is illustrated in Fig. 3, where  $-P_{\max}$  is the maximum power absorption at BESS 1, and  $+P_{\max}$  is the maximum power injection at BESS 2.

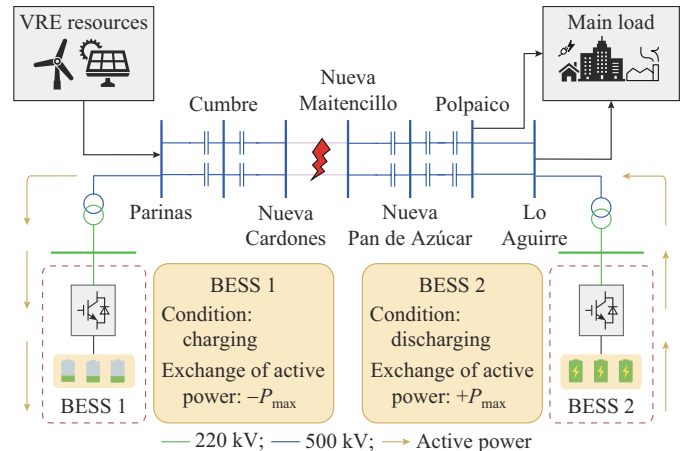


Fig. 3. Schematic diagram of contingency operation.

### B. GB EMT Model

A simplified diagram of the BESS modeled in the EMT-NPG is presented in Fig. 4. It consists of a converter represented by a voltage source converter (VSC) average value model (AVM) [21] and supplied by a constant DC voltage source ( $v_{dc}$ ). On the AC side, the converter is connected to a filter and a step-up transformer that interfaces the BESS with the grid at the point of connection (POC).

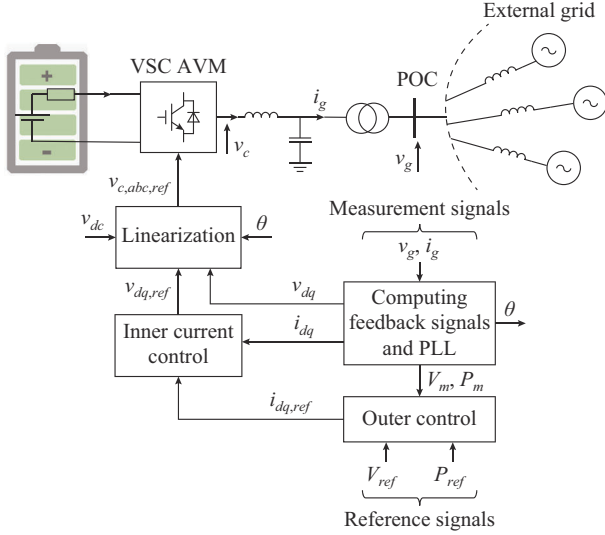


Fig. 4. Block diagram of BESS model.

The architecture of GB control system presented in Fig. 5 corresponds to a cascaded control structure that includes an inner current control represented in the synchronous rotating  $dq0$  reference frame [22]. The inner current control contains a proportional-integral controller, feedforward decoupling terms, and current limiters. The output of the  $dq0$ - $abc$  linear transformation determines the voltage reference signal  $v_{c,abc,ref}$  for the modulator of the converter. The outer control loop contemplates the references for active power control and AC voltage/reactive power ( $V/Q$ ) control ( $P_{ref}$ ,  $V_{ref}$ ) and provides current references  $i_{dq,ref}$  for the inner current control loop. The instantaneous voltage and current signals at the POC ( $v_g$ ,  $i_g$ ) are used to determine the measured power  $P_m$  and voltage  $V_m$ , as well as the voltages  $v_{dq}$  and currents  $i_{dq}$  in the  $dq0$  reference frame from the angle  $\theta$  provided by the phase-locked loop (PLL) [23]. A fault ride-through (FRT) mode is activated when voltage drops below a certain threshold ( $FRT_{ON}$ ) and is deactivated once the voltage is recovered ( $FRT_{OFF}$ ). In this mode, the reactive current of the converter is proportional to the voltage deviation from the nominal value.

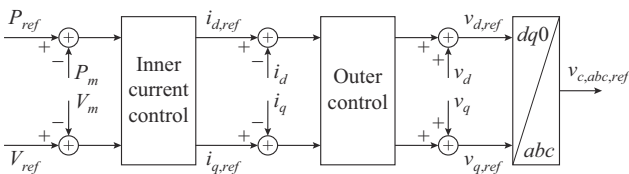


Fig. 5. Architecture of GB control system.

The active power output in the converter can be linearly

ramped from 0 to the maximum power of 500 MW once the activation signal is received using a settable ramp rate in MW/s. The activation signal for the converters is generated 100 ms after fault clearance in the 500 kV corridor, represented by the communication delay  $t_{act}$ . The main parameters of GB are detailed in Table III, where  $SoC_{max}$  and  $SoC_{min}$  are the maximum and minimum SoC limits, respectively; and  $R_{BESS}$  is the series resistance of the DC source.

TABLE III  
MAIN PARAMETERS OF GB

Parameter	Value	Parameter	Value
Capacity	125 MWh	Power	500 MVA
$v_{dc}$	25 kV	$R_{BESS}$	1 n $\Omega$
$SoC_{max}$	0.95 p.u.	$SoC_{min}$	0.05 p.u.

The reference active power  $P_{ref}$  is defined as:

$$P_{ref} = \begin{cases} 0 & t \leq t_{act} \\ \min\{P_{max}, P_{max}(t - t_{act})r_{gb}\} & t > t_{act} \end{cases} \quad (1)$$

where  $P_{max}$  is set to be 500 MW, and the ramp rate  $r_{gb}$  can take different values depending on the specific scenario under consideration.

## IV. SIMULATION RESULTS

This section presents the simulation results for different contingencies. The goal is to assess the dynamic behavior and performance of the GB under fault conditions.

### A. Methodology

The analysis aims to evaluate the dynamic behavior of the GB and to define the specifications and technical requirements for key performance features. The following aspects of the GB control system are assessed.

- 1) Active power ramp rate to keep the grid stable.
- 2) Short-term overload.
- 3) Power factor range and dynamic reactive power compensation during and after faults.

The analysis is comprised of the following two stages.

1) Preliminary contingency case simulations: identify the worst case by simulating  $N-1$  contingencies across the 500 kV corridor with different active power ramp rates in MW/s. Twelve two-phase-to-ground (2PG) faults, at each 500 kV line section, are simulated. An example of fault location is shown in Fig. 3.

2) Worst-case simulations: for the worst case identified in the previous stage, simulations are performed considering different active power ramp rates in MW/s and FRT limits for the dynamic reactive power compensation devices near the 500 kV corridor. The goal is to identify the critical parameter and control setpoints required to keep the NPG stable in compliance with the performance requirements in the grid code.

All time-domain EMT simulations are initialized from the multiphase load-flow solver available in EMTP<sup>®</sup>. The details of these stages are presented in the following.

B. Preliminary Contingency Cases

The preliminary contingency cases evaluated, considering fixed FRT limits of the reactive power compensator ( $FRT_{ON}=0.1$ ,  $FRT_{OFF}=0.075$ ), are summarized in Table IV.

TABLE IV  
SUMMARY OF PRELIMINARY CONTINGENCY CASES

Case	Scenario	Active power ramp rate of BESS (MW/s)
1	1	50
2	1	500
3	2	50
4	2	500

Twelve faults at different locations in the 500 kV corridor were analyzed for each case, as shown in Table V, to assess the system dynamic behavior and performance. Only six busbars with the largest voltage magnitude deviation and slower post-fault recovery rate are presented, along with the frequency at the Polpaico busbar. Additionally, the active and reactive power outputs of the BESS units and power flow variation in the lines for the worst case are also presented.

TABLE V  
FAULT LOCATIONS IN 500 kV CORRIDOR

Fault	Line	Location
F1	Parinas–Cumbre	North
F2	Parinas–Cumbre	South
F3	Cumbre–Nueva Cardones	North
F4	Cumbre–Nueva Cardones	South
F5	Nueva Cardones–Nueva Maitencillo	North
F6	Nueva Cardones–Nueva Maitencillo	South
F7	Nueva Maitencillo–NPA	North
F8	Nueva Maitencillo–NPA	South
F9	NPA–Polpaico	North
F10	NPA–Polpaico	South
F11	Polpaico–Lo Aguirre	North
F12	Polpaico–Lo Aguirre	South

Based on the preliminary contingency case simulations, fault F10 occurring within the 500 kV segment NPA–Polpaico, as shown in Fig. 6, is identified as the most critical contingency.

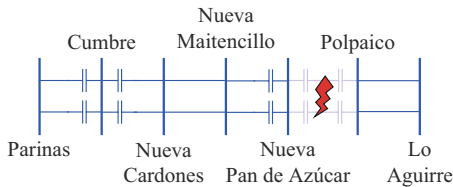


Fig. 6. Worst case for all preliminary contingency cases.

Cases 1 and 2: both cases exhibit clear signs of instability. This is illustrated in Fig. 7 for Case 1, where an unstable voltage at Cumbre busbar, and the frequency with significant oscillations at Polpaico busbar are observed for fault F10.

Similarly, in Case 2, the unstable nature of fault F10 and the lack of voltage and frequency stabilization at the designated busbars are confirmed by Fig. 8.

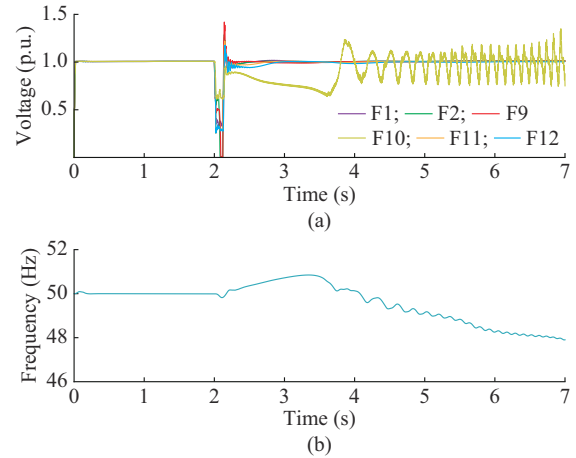


Fig. 7. Voltages and frequency for Case 1. (a) Voltages at Cumbre busbar. (b) Frequency at Polpaico busbar under fault F10.

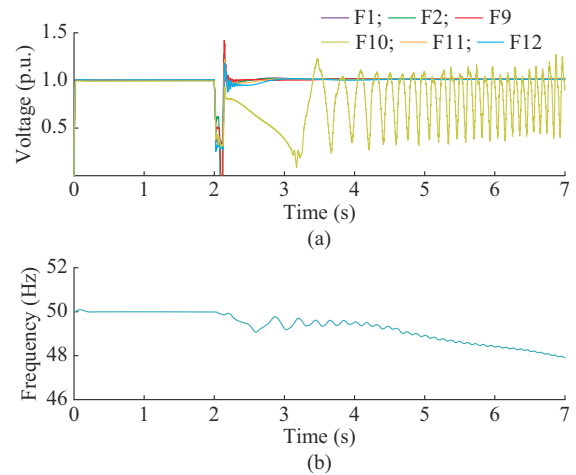


Fig. 8. Voltages and frequency for Case 2. (a) Voltages at Cumbre busbar. (b) Frequency at Polpaico busbar under fault F10.

Cases 3 and 4: in these two cases, the simulations are fully stable and comply with the requirements of the grid code. As shown in Fig. 9(a) and Fig. 10(a), voltages exhibiting the most significant oscillations are effectively stabilized, and the amplitude of such oscillations is not very large. Furthermore, as observed in Fig. 9(b) and Fig. 10(b), a small frequency oscillation occurs, which is well-damped.

From Fig. 11(a) and Fig. 12(a), it is clear that the GB exhibits the expected dynamic behavior according to the predefined ramp rates. Besides, when comparing the active power flow on the NPA–Polpaico line in Fig. 11(b) and Fig. 12(b), it can be observed that in the case where the ramp rate is higher, the active power transfer in circuit 1 (C1) stabilizes more quickly.

Judging by the results of the preliminary contingency cases, the worst case is the fault F10, located at the end of Polpaico busbar. It is the only fault that always leads to instability in scenario 1. Therefore, it was used for the worst-case analysis.

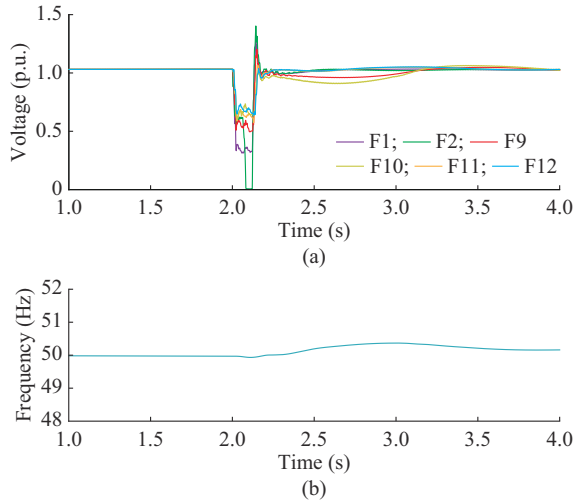


Fig. 9. Voltage and frequency for Case 3. (a) Voltages at Cumbre busbar. (b) Frequency at Polpaico busbar under fault F10.

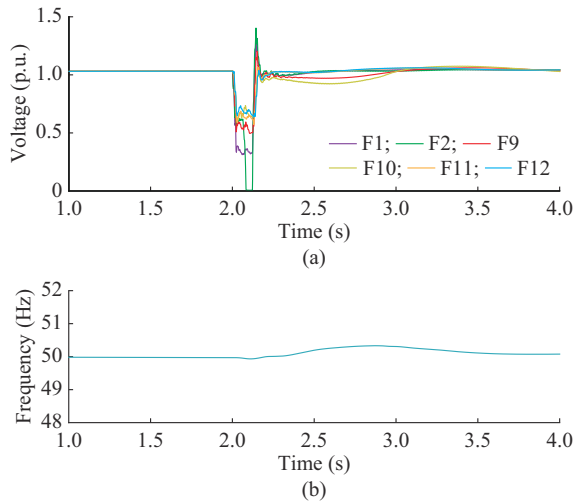


Fig. 10. Voltages and frequency for Case 4. (a) Voltages at Cumbre busbar. (b) Frequency at Polpaico busbar under fault F10.

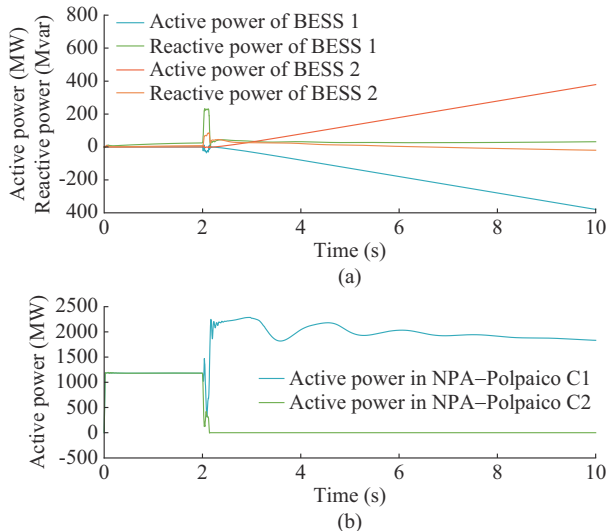


Fig. 11. GB power injection and active power transfer on NPA-Polpaico line for Case 3 under fault F10. (a) GB power injection. (b) Active power transfer on NPA-Polpaico line.

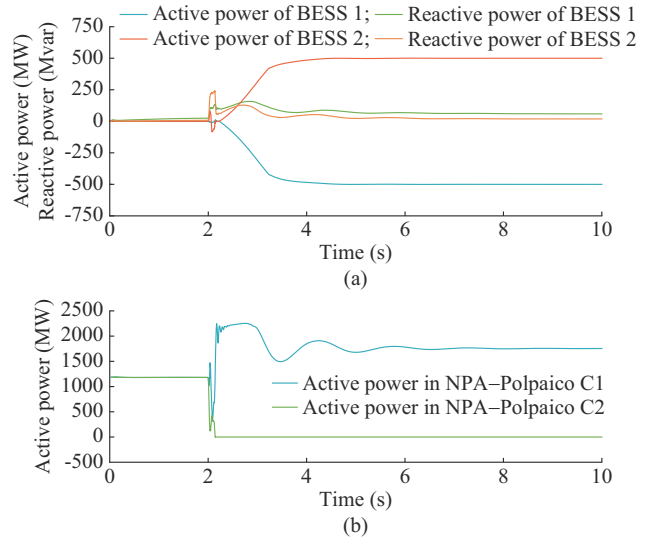


Fig. 12. GB power injection and active power transfer on NPA-Polpaico line for Case 4 under fault F10. (a) GB power injection. (b) Active power transfer on NPA-Polpaico line.

C. Worst Case

This subsection presents an extended analysis of the worst case (fault F10) for scenario 1. Modifications will be made to the FRT limits of the reactive power compensator presented in the system. Additionally, variations will be introduced to the active power ramp rates in the response of the BESS. The specifics of these variations can be found in Table VI.

TABLE VI  
SUMMARY OF WORST-CASE CONDITIONS

Condition	Active power ramp rate of BESS (MW/s)	FRT limits (p.u.)			
		GB		Compensator	
		$FRT_{ON}$	$FRT_{OFF}$	$FRT_{ON}$	$FRT_{OFF}$
WC1	50	0.2	0.200	0.5	0.075
WC2	1000	0.2	0.075	0.1	0.075
WC3	500	0.2	0.075	0.1	0.075

1) Worst-case condition 1 (WC1): the system remains stable under this condition, as shown in Fig. 13. When examining the voltage waveforms at specific busbars, it is evident that despite large fluctuations, the grid remains stable and maintains synchronism, and the same happens with the system frequency.

Altering the FRT limits requires reactive power compensators to stay connected even under more extreme conditions beyond stable operation. This ensures that voltage levels remain within the range specified by the grid code, maintaining the system stability even when the active power ramp rate is 50 MW/s, as illustrated in Fig. 14(a). The waveform in Fig. 14(b) demonstrates that the active power transfers on the NPA-Polpaico line presents a correct behavior.

2) Worst-case condition 2 (WC2): as illustrated in Fig. 15, the system remains stable under this condition. A close look at the voltage waveforms for selected busbars reveals that, even some initial oscillations occur, the grid successfully preserves its synchronism, and a similar phenomenon is observed in the system frequency.

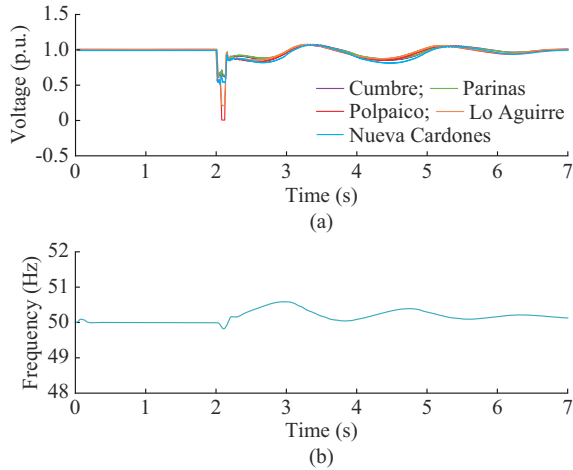


Fig. 13. Voltages and frequency for WC1. (a) Voltages at different busbars. (b) Frequency at Polpaico busbar.

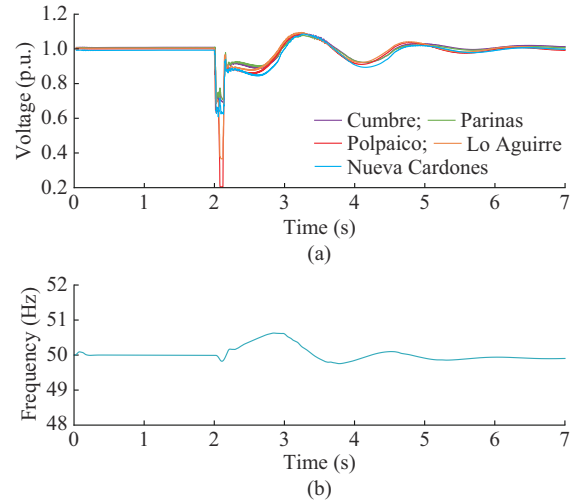


Fig. 15. Voltages and frequency for WC2. (a) Voltages at different busbars. (b) Frequency at Polpaico busbar.

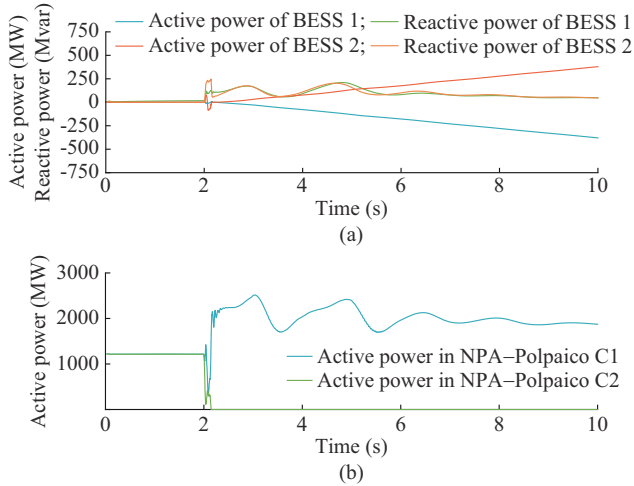


Fig. 14. GB power injection and active power transfer on NPA-Polpaico line for WC1. (a) GB power injection. (b) Active power transfer on NPA-Polpaico line.

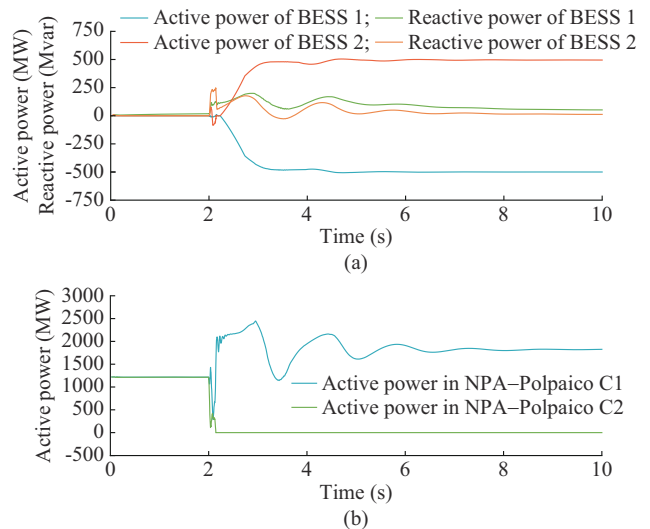


Fig. 16. GB power injection and active power transfer on NPA-Polpaico line for WC2. (a) GB power injection. (b) Active power transfer on NPA-Polpaico line.

An important improvement is observed with the increase of the active power ramp rate, as shown in Fig. 16(a). The increase of the active power ramp rate facilitates the system stability without altering the initial FRT limits of reactive power compensators and expedites active power stabilization on the NPA-Polpaico corridor, as shown in Fig. 16(b). However, this ramp rate is now twentyfold compared with WC1, potentially impacting the battery lifespan.

3) Worst-case condition (WC3): under this condition, a voltage dip below 0.8 p.u., at certain busbars, violates the grid code. Although frequency is not the primary issue, a slight over-frequency occurs when compared with WC2, as observed in Fig. 17. As for the behavior of the GB, an undesirable active power response can be observed in Fig. 18.

V. CONCLUSION

This paper provides an analysis of the impact of the GB project on the Chilean NPG using EMT simulations. Key findings of this study are as follows:

1) The GB increases the transmission capacity and maintains the system stability.

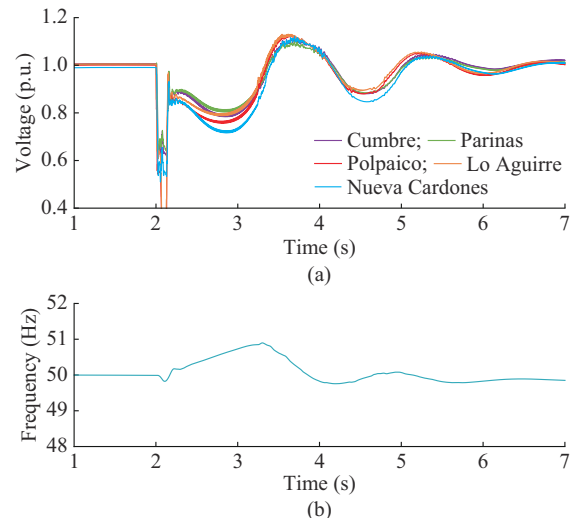


Fig. 17. Voltages and frequency for WC3. (a) Voltages at different busbars. (b) Frequency at Polpaico busbar.

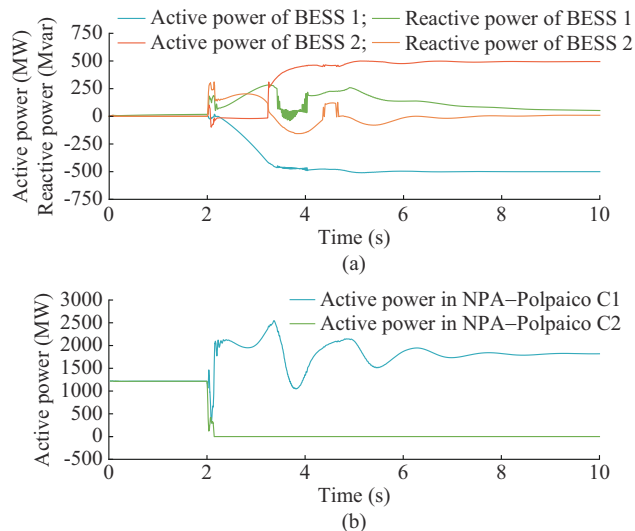


Fig. 18. GB power injection and active power transfer on NPA-Polpaico line for WC3. (a) GB power injection. (b) Active power transfer on NPA-Polpaico line.

2) FRT limits of reactive power compensators are critical to grid stability. Large FRT limits ensure that voltages are kept within the requirements of the grid code, while lower limits require higher active power ramp rates.

3) This study introduces the first wide-area EMT model for the NPG, unlocking new opportunities for advanced and complex time-domain stability analyses and research.

These findings reinforce the effectiveness of the GB and contribute valuable guidelines for implementing innovative solutions.

Future work may consider the assessment and impact of incorporating grid-forming capabilities in the BESS to support and improve system stability, as well as supplementary features and capabilities such as damping oscillations, voltage unbalance and harmonics compensation, and resonance mitigation.

## REFERENCES

- [1] CEN. (2023, May). Chilean Independent System Operator. [Online]. Available: <https://www.coordinador.cl>
- [2] F. Arraño-Vargas and G. Konstantinou, "Longitudinal power systems for modern and future grid studies: a graph theory analysis," *Sustainable Energy, Grids and Networks*, vol. 35, p. 101132, Sept. 2023.
- [3] CEN. (2022, Jun.). Roadmap for an accelerated energy transition: vision of the Chilean system operator. [Online]. Available: <https://www.coordinador.cl>
- [4] J. Porst, J. Richter, G. Mehlmann *et al.*, "Operation of grid boosters in highly loaded transmission grids," in *Proceeding of 2022 IEEE International Conference on Power Systems Technology*, Kuala Lumpur, Malaysia, Sept. 2022, pp. 1-6.
- [5] CNE. (2019, Jun.). NTSyCS, Chilean grid code. [Online]. Available: <https://www.cne.cl>
- [6] M. Lindner, D. Mende, A. Wasserrab *et al.*, "Corrective congestion management in transmission grids using fast-responding generation, load and storage," in *Proceeding of 2021 IEEE Electrical Power and Energy Conference*, Toronto, Canada, Oct. 2021, pp. 1-6.
- [7] T. A. Nguyen and R. H. Byrne, "Evaluation of energy storage providing virtual transmission capacity," in *Proceeding of 2021 IEEE PES General Meeting*, Washington DC, USA, Jul. 2021, pp. 1-5.
- [8] CNE. (2021, Aug.). 2021 transmission expansion plan. [Online]. Available: <https://www.cne.cl>
- [9] P. Kundur, *Power System Stability and Control*. New York: McGraw-Hill, 1994.

- [10] F. Arraño-Vargas and G. Konstantinou, "Development of real-time benchmark models for integration studies of advanced energy conversion systems," *IEEE Transactions on Energy Conversion*, vol. 35, no. 1, pp. 497-507, Mar. 2020.
- [11] F. Milano, F. Dorfler, G. Hug *et al.*, "Foundations and challenges of low-inertia systems," in *Proceeding of 2018 Power Systems Computation Conference*, Dublin, Ireland, Jun. 2018, pp. 1-25.
- [12] J. D. Lara, R. Henriquez-Auba, D. Ramasubramanian *et al.*, "Revisiting power systems time-domain simulation methods and models," *IEEE Transactions on Power Systems*. doi: 10.1109/TPWRS.2023.3303291
- [13] M. Ouafi, J. Mahseredjian, J. Peralta *et al.*, "Parallelization of EMT simulations for integration of inverter-based resources," *Electric Power Systems Research*, vol. 223, p. 109641, Oct. 2023.
- [14] J. Mahseredjian, V. Dinavahi, and J. A. Martinez, "Simulation tools for electromagnetic transients in power systems: overview and challenges," *IEEE Transactions on Power Delivery*, vol. 24, no. 3, pp. 1657-1669, Jul. 2009.
- [15] U. Karaagac, J. Mahseredjian, and O. Saad, "An efficient synchronous machine model for electromagnetic transients," *IEEE Transactions on Power Delivery*, vol. 26, no. 4, pp. 2456-2465, Oct. 2011.
- [16] P. Pourbeik. (2018, Jul.). Model user guide for generic renewable energy system models, EPRI. [Online]. Available: <https://www.epri.com/research/products/00000003002014083>
- [17] P. Pourbeik, J. J. Sanchez-Gasca, J. Senthil *et al.*, "Generic dynamic models for modeling wind power plants and other renewable technologies in large-scale power system studies," *IEEE Transactions on Energy Conversion*, vol. 32, no. 3, pp. 1108-1116, Sept. 2017.
- [18] WECC Renewable Energy Modeling Task Force. (2014, Jan.). WECC wind plant dynamic modeling guidelines. [Online]. Available: <https://www.esig.energy/wiki-main-page/wind-plant-power-flow-modeling-guide/>
- [19] H. Dommel, "Digital computer solution of electromagnetic transients in single-and multiphase networks," *IEEE Transactions on Power Apparatus and Systems*, vol. PAS-88, no. 4, pp. 388-399, Apr. 1969.
- [20] CEN. (2023, Jun.). BESS functional technical specifications. [Online]. Available: <https://www.coordinador.cl>
- [21] H. Saad, S. Denetiere, J. Mahseredjian *et al.*, "Modular multilevel converter models for electromagnetic transients," *IEEE Transactions on Power Delivery*, vol. 29, no. 3, pp. 1481-1489, Jun. 2014.
- [22] A. Yazdani and R. Iravani, *Voltage-sourced Converters in Power Systems*. Hoboken: Wiley, 2010.
- [23] S. Golestan, J. M. Guerrero, and J. C. Vasquez, "Three-phase PLLs: a review of recent advances," *IEEE Transactions on Power Electronics*, vol. 32, no. 3, pp. 1894-1907, Mar. 2017.

**Matías Agüero** received his B.Sc. and M.Sc. degrees in electrical engineering from the University of Chile, Santiago, Chile, in 2023. He is currently working as Power Systems Studies Engineer at Coordinador Eléctrico Nacional, the Chilean System Operator, Santiago, Chile. His research interests include power system modeling and control, power system stability, and artificial intelligence applications for power system stability.

**Jaime Peralta** received his B.Sc. degree in electrical engineering from the University of Chile, Santiago, Chile, in 1994, his M.A.Sc. and Ph.D. degrees from the École Polytechnique de Montréal, Montréal, Canada, in 2007 and 2012, respectively. He has held technical and management positions in different companies in North America including BC Hydro, Siemens Canada, and Alstom Grid US. He is currently Director at Coordinador Eléctrico Nacional, the Chilean System Operator, Santiago, Chile. His research interests include integration of renewable generation, transmission planning, design of flexible AC transmission system (FACTS) and high-voltage direct current (HVDC) systems.

**Eugenio Quintana** received his B.Sc. degree in electrical engineering from the University of Chile, Santiago, Chile, in 2012. From 2012 to 2014, he worked in Systep. He currently works as Head of the Power System Studies Department at Coordinador Eléctrico Nacional, the Chilean System Operator, Santiago, Chile. His research interests include power system stability and electromagnetic transient (EMT) analysis.

**Victor Velar** received his B.Sc. degree in electrical engineering from the Pontificia Universidad Católica de Chile, Santiago, Chile. From 2000 to 2015, he worked in the ENDESA-ENEL conglomerate, where he was Head of the Electrical Transmission Studies Area for Latin America. He currently

works at Coordinador Eléctrico Nacional, the Chilean System Operator, Santiago, Chile, as Deputy Manager of studies and real-time simulation. His research interests include power system stability and EMT analysis.

**Anton Stepanov** received his B.Sc. degree in electrical and power systems from the South Ural State University, Chelyabinsk, Russia, in 2013, his M.Sc. degree in electronic systems and electrical engineering from the École Polytechnique de l'Université de Nantes, Saint-Nazaire, France, in 2015, and his Ph.D. degree in electrical engineering from the École Polytechnique de Montréal, Montréal, Canada, in 2020. Since 2020, he has been with PG-STEch, Montreal, Canada. His research interests include HVDC systems modeling, analysis, and simulation.

**Hossein Ashourian** received his Ph.D. degree from the Concordia University, Montreal, Canada, in 2018. Since 2018, he has been with EMTP as a Senior Engineer and Developer. His research interests include renewable resource integration, and power system modeling and simulation.

**Jean Mahseredjian** received his Ph.D. degree from École Polytechnique de Montréal, Montréal, Canada, in 1991. From 1987 to 2004, he was with IREQ (Hydro-Quebec), working on research and development activities related to the simulation and analysis of EMT. In December 2004, he joined the Faculty of Electrical Engineering with École Polytechnique de Montréal, where he is currently a Professor. He is IEEE Fellow for his contributions to the computation and modeling of power systems transients. His research interests include power system stability and control, power electronics, and EMT.

**Roberto Cárdenas** received his B.Sc. degree in electrical engineering from the University of Magallanes, Punta Arenas, Chile, in 1988, and his M.Sc. degree in electronic engineering, and his Ph.D. degree in electrical and electronic engineering from the University of Nottingham, Nottingham, U.K., in 1992 and 1996, respectively. He is currently a Professor of power electronics and drives with the Electrical Engineering Department, University of Chile, Santiago, Chile. His research interests include power system modeling, stability and control, and power electronics.